Available online at www.sciencedirect.com
SCIENCE DIRECT®
International Journal of Mass Spectrometry 227 (2003) 509–524
International Journal of Mass Spectrometry
www.elsevier.com/locate/ijms

The Na^+ affinities of α-amino acids: side-chain substituent effects

Michelle M. Kish[a], Gilles Ohanessian[b], Chrys Wesdemiotis[a,*]

[a] *Department of Chemistry, The University of Akron, Akron, OH 44325, USA*
[b] *Laboratoire des Mécanismes Réactionnels, UMR 7651 du CNRS, Ecole Polytechnique, F-91128 Palaiseau Cedex, France*

Received 28 March 2002; accepted 15 August 2002

Abstract

Na^+-bound heterodimers of amino acids (AA) are produced in the gas phase by electrospray ionization (ESI). The dissociation kinetics of these AA_1–Na^+–AA_2 ions are determined by collisionally activated dissociation (CAD) and converted to a ladder of relative Na^+ affinities via the Cooks kinetic method. The affinities derived follow the order (kJ mol^{-1}, relative to Gly): Gly (0), Ala (6), Val (12), Leu (13), Cys (14), Ile (15), Ser (31), Pro (35), Thr (36), Phe (37), Tyr (40), Asp (42), Glu (43), Asn (45), Trp (49), Gln (51), His (57). Absolute Na^+ binding energies are estimated by anchoring the relative values to the Na^+ affinity of Ala (167 kJ mol^{-1}), measured by the same approach using Na^+-bound dimers of Ala and a series of acetamide derivatives. The Na^+ binding energies of the acetamide reference bases and of representative aliphatic and side-chain functionalized amino acids (Gly, Ala, Pro, Cys and Ser) are determined by ab initio theory. Experimental and ab initio affinities agree very well. The combined data show that functional side chains increase the AA–Na^+ bond strength by providing an extra ligand to the metal ion. Aromatic and carbonyl substituents in the side chain bring about substantial increases in the Na^+ binding energy, with particularly large increments observed for amide and electron-rich (N-containing) aromatic groups. A poor correlation is found between sodium ion and proton affinities, strongly suggesting that the Na^+ complexes do not have salt-bridge structures involving zwitterionic amino acids (in which the most basic site is protonated).

Keywords: Amino acids; Sodium ion affinities; Kinetic method; Charge solvation; Salt bridge

1. Introduction

Sodium ion is one of the most abundant metal ions in biological systems, where it is involved in a variety of processes, including osmotic balance, the stabilization of biomolecular conformations and information transfer via ion pumps and ion channels [1–4]. Na^+ interacts with peptides and proteins to perform such regulatory and structural functions. For a better understanding of these interactions, information about the intrinsic binding modes of Na^+ to appropriate, simple model systems is necessary. The present study addresses this subject by using the kinetic method developed by Cooks and coworkers [5,6] to determine the thus far largely unknown relative Na^+ affinities of α-amino acids, the building blocks of peptides and proteins.

The thermochemistry and structures of the Na^+ complexes of the α-amino acids (AA) glycine (Gly),

* Corresponding author. Tel.: +1-330-972-7699; fax: +1-330-972-7370.
E-mail address: wesdemiotis@uakron.edu (C. Wesdemiotis).

1387-3806/03/$ – see front matter © 2003 Elsevier Science B.V. All rights reserved.
doi:10.1016/S1387-3806(03)00082-4

alanine (Ala), proline (Pro), serine (Ser), cysteine (Cys), phenylalanine (Phe), tyrosine (Tyr), tryptophan (Trp) and arginine (Arg) have been examined by ab initio and/or density functional theory [7–20]. These investigations showed that the most stable $[AA + Na]^+$ isomers generally result from charge solvation of Na^+ by the carbonyl oxygen, amine nitrogen and, if present, side-chain functional group of AA. Pro (a secondary amino acid) deviates from this behavior, favoring the formation of a salt bridge, in which Na^+ is bound between the O atoms of the carboxylate group, while carboxylate and ammonium centers interact through a hydrogen bond [13,20]. With amino acids other than Pro, such zwitterionic geometries lie higher in energy than charge-solvated geometries, except for Arg, where both types of Na^+ complexation have approximately equal energetics [14]. Based on the computational studies reported thus far, Na^+ affinities increase from aliphatic to side-chain functionalized amino acids because of the extra ligand provided by the side chain [13,16,17,20]. Within aliphatic $[AA + Na]^+$ complexes, the Na^+ binding energy is augmented with increasing substituent size at the α-carbon and whenever salt bridges can be formed (e.g., with Pro) [15,18,20].

Limited experimental data are available about the binding energy of Na^+ to amino acids. In an early study, Bojesen et al. used the Cooks kinetic method to deduce the order of Na^+ affinities of the common α-amino acids based on the dissociation kinetics of Na^+-bound heterodimers $AA_1–Na^+–AA_2$, where AA_1 and AA_2 represent two different amino acids [21]. Actual Na^+ affinities were given only for Gly, Val, sarcosine (*N*-methyl glycine), glycine methylester and α-aminobutyric acid based on their relative affinities vs. Ala, whose Na^+ binding energy was estimated at 75% of the Ala–Li^+ bond energy. A later study by Kebarle and coworkers determined the absolute sodium ion affinity (ΔH_{298}) of Gly by threshold collision-induced dissociation (153 kJ mol^{-1}) [22]. More recently, a kinetic method investigation by Cerda and coworkers derived the Na^+ affinities of Phe (174), Tyr (175) and Trp (180 kJ mol^{-1}) [17]. The increments between Phe, Tyr, and Trp were in fair agreement with predictions by DFT calculations but the relative affinity between Phe (174) [17] and the value reported by Bojesen et al. for Ala (165 kJ mol^{-1}) [21] was markedly smaller than the increment indicated by theory (31 kJ mol^{-1}) [16,17]. Gapeev and Dunbar reexamined the thermochemistry of the Ala–Na^+ and Phe–Na^+ bonds via ligand-exchange equilibrium measurements and anchored these affinities to the well-known Na^+ affinity of pyridine, which led to ΔH_{298} values of 159 and 188 kJ mol^{-1} for Ala and Phe, respectively [23]. The relative or absolute energetics of other AA–Na^+ bonds remain unknown.

Concerning the structures of $[AA + Na]^+$ complexes, ion mobility experiments on sodiated glycine and methylated analogs were unable to distinguish between charge-solvated and zwitterionic structures, both of which are predicted to have nearly identical collision cross sections [15]. Insight on this topic was provided by the dissociation characteristics of Na^+-bound dimers of fifteen α- and two β-amino acids and the corresponding methyl esters, $AA–Na^+–AAOCH_3$, which revealed the Na^+ affinity order $AA < AAOCH_3$ for the examined amino acids besides Pro [20,24]. These trends corroborated the computational prediction that most AA molecules bind sodium ion via charge solvation (i.e., with the AA ligand as a free acid), except for Pro which binds Na^+ with its zwitterionic form in a salt bridge arrangement [10,13,16,20]. Since AA methyl esters are incapable of forming zwitterions but are more basic than AA due to the electron-donating properties of the methyl group [25], a Na^+ affinity increase from AA to $AAOCH_3$ is indicative of charge solvation in the $[AA + Na]^+$ complex [20,24]. Conversely, the Na^+ affinity decrease from Pro to $ProOCH_3$ is diagnostic of a salt bridge in $[Pro + Na]^+$; the salt bridge is disabled in $[ProOMe + Na]^+$, thereby removing attractive ionic interactions, which in turn lowers the Na^+ binding energy [20,24].

The computational and experimental studies described clearly show that knowledge of the energetics of the AA–Na^+ bonds renders not only fundamental thermochemical information but also structural information about the $[AA + Na]^+$ complexes. In this

investigation, we combine experimental and quantum chemistry methods to determine the energetics of Na^+ binding to seventeen common α-amino acids, in order to evaluate the dependence of binding energy on the side-chain substituents. Relative affinities are measured by applying the kinetic method to AA_1–Na^+–AA_2 heterodimers produced by electrospray ionization (ESI) [26,27]. The relative scale is anchored to the Na^+ affinity of Ala, which is reinvestigated by using Na^+-bound dimers of Ala and a series of acetamides as reference bases. The Na^+ binding energies of the acetamides are established by ab initio theory. New Na^+ binding energies of selected amino acids (Gly, Ala, Pro, Cys and Ser) are also calculated at the ab initio level for comparison with and evaluation of the experimental results.

2. Methods

2.1. Experimental

All experiments were performed with a Bruker Esquire-LC ion trap mass spectrometer (Billerica, MA) equipped with an ESI ion source. The ESI solvent used was a 2:1 mixture of water and methanol. For the formation of AA_1–Na^+–AA_2 dimers, 1 mg each of amino acid and sodium trifluoroacetate was dissolved in 1 mL of solvent. The solutions were combined in the ratio AA_1:AA_2:salt = 1:1:0.75 and the resulting mixture was introduced into the ion source at the rate of 240–300 μL/h by means of a syringe pump. The entrance of the sampling capillary, which is orthogonal to the grounded spraying needle, was set at −4 kV. Nitrogen was used as the nebulizing gas (10 psi) and drying gas (8 L/min, 160 °C). Collisionally activated dissociation (CAD) tandem mass spectra of AA_1–Na^+–AA_2 were measured by isolating the heterodimer ions and exciting them to fragment with a radiofrequency (RF) that was resonant with their frequency of motion in the trap [28]. The precursor ions absorb energy and are accelerated in this process, thus undergoing CAD with the He buffer gas in the trap. The excitation time was 40 ms and the RF amplitude (V_{p-p}) was adjusted within 0.55 ± 0.17 V to optimize the fragment ion yield. Thirty scans were averaged per spectrum and the experiments were replicated 2–3 times to determine the standard deviation of relative abundances. An analogous procedure was followed for the acquisition of the CAD spectra of Ala–Na^+–B_i (B_i = aliphatic amides), which were measured at four distinct collision energies, corresponding to V_{p-p} amplitudes of 0.4, 0.5, 0.6 and 0.7 V. The amino acids, amides, solvents and sodium trifluoroacetate were purchased from Sigma or Aldrich (Milwaukee, WI) and were used in the condition received.

2.2. Kinetic method

$$AA_1\text{–}Na^+ + AA_2 \overset{k_1}{\leftarrow} AA_1\text{–}Na^+\text{–}AA_2 \overset{k_2}{\rightarrow} AA_1 + Na^+\text{–}AA_2 \quad (1)$$

$$\ln\left(\frac{k_1}{k_2}\right) = -\frac{[\Delta G_1^{\ddagger} - \Delta G_2^{\ddagger}]}{RT_{\text{eff}}} = \frac{[\Delta S_1^{\ddagger} - \Delta S_2^{\ddagger}]}{R} - \frac{[\Delta H_1^{\ddagger} - \Delta H_2^{\ddagger}]}{RT_{\text{eff}}} \quad (2)$$

$$\ln\left(\frac{k_1}{k_2}\right) = -\frac{[\Delta S_{\text{Na}}^{\text{app}}(AA_1) - \Delta S_{\text{Na}}^{\text{app}}(AA_2)]}{R} + \frac{\Delta H_{\text{Na}}(AA_1) - \Delta H_{\text{Na}}(AA_2)}{RT_{\text{eff}}} = -\frac{\Delta(\Delta S_{\text{Na}})^{\text{app}}}{R} + \frac{\Delta H_{\text{Na}}(AA_1) - \Delta H_{\text{Na}}(AA_2)}{RT_{\text{eff}}} \approx \frac{\Delta H_{\text{Na}}(AA_1) - \Delta H_{\text{Na}}(AA_2)}{RT_{\text{eff}}} \quad (3)$$

The CAD spectra of AA_1–Na^+–AA_2 show dominant fragment ions arising from dissociation of the heterodimer into the individual metalated monomers, Eq. (1). The abundance ratio of the AA_1–Na^+ and Na^+–AA_2 peaks in a given spectrum represents an approximate measure of the rate constant ratio of the dissociations leading to these fragment ions, k_1/k_2.

This assumption presupposes that other competing pathways and mass discrimination effects are negligible. Based on the thermodynamic formulation of transition state theory [29], the natural logarithm of k_1/k_2 is a function of the relative free energy of activation of the two competing dissociations of the heterodimer, as shown in Eq. (2), where R is the ideal gas constant and T_{eff} is the effective temperature of the dissociating dimer ions [30]. The free energies encompass the enthalpy and entropy components included in Eq. (2). The unimolecular reactions of Eq. (1) involve cleavages of electrostatic bonds, which generally proceed without appreciable reverse activation energy [21,22,31–34]. In such cases, the relative enthalpy of activation becomes equivalent to the difference in binding enthalpies of Na^+ to AA_1 and AA_2, cf. Eq. (3) [the binding enthalpy, also called binding energy or affinity in this study, is defined as the enthalpy change, ΔH, of the reaction [$AA–Na^+ \rightarrow AA + Na^+$]. Further, the relative activation entropy is replaced with an apparent relative entropy of activation of the $AA_1–Na^+$ and $AA_2–Na^+$ bonds (for simplicity, also called apparent relative entropy or difference in the apparent Na^+ binding entropies of AA_1 and AA_2). The use of an effective temperature and apparent entropy difference in place of a thermodynamic temperature and entropy difference reflects the fact that the Na^+-bound dimers have non-Boltzmann energy distributions and are not in thermal equilibrium with their surroundings. Recent studies by Ervin [35] and us [36] have revealed that $\Delta(\Delta S^{app})$ depends on the identity of the decomposing dimer ion and on T_{eff} and can range from ~0 to the corresponding actual (i.e., thermodynamic) entropy difference $\Delta(\Delta S)$ of the $AA_1–Na^+$ and $AA_2–Na^+$ bonds. If the apparent entropies of Na^+ attachment to AA_1 and AA_2 are comparable, which will be shown to be true for most molecules compared here (vide infra), Eq. (3) is simplified as shown, now linking directly the experimental k_1/k_2 ratios to the relative Na^+ affinities of the amino acids compared in the heterodimers. Affinities, which are much less dependent on temperature than free energies [37], are more suitable for establishing correlations between intrinsic thermochemistry and specific structural features, especially in kinetic method studies where the actual temperature of the ions under study is poorly defined [5,6,30].

The examination of $AA_1–Na^+–AA_2$ dimers provides relative affinities. Absolute ΔH data can also be obtained if the relative values are anchored to an amino acid of known Na^+ binding energy. The anchoring ΔH value can be determined by the same procedure, from the dissociation kinetics of heterodimers $AA–Na^+–B_i$ that are composed of the anchor (AA) and reference bases of well established affinity (B_i). This approach has successfully been used in the measurement of proton [38,39], Cu^+ [40–42] and Ag^+ [43] affinities of amino acids.

2.3. Calculations

The calculations of binding enthalpies were carried out following procedures which have been described and used previously. The geometries of the neutral ligands and sodiated complexes were determined by full optimization followed by a vibrational frequency analysis, both at the MP2(full)/6-31G* level, where "(full)" indicates that there were no electrons frozen in the MP2 calculations. Final energetics were obtained at the MP2(full)/6-311+G(2d,2p) level using the MP2/6-31G* geometries. Previous work has shown that Na^+ binding energies of various small and medium-sized molecules computed at this level are accurate, probably due to a cancellation of (small) errors [13,44]. No basis set superposition error (BSSE) correction was applied to the results [45]. Zero-point vibrational energies and thermal corrections at 298 K were obtained from the vibrational analysis and used to derive the 298 K binding enthalpies reported. Binding entropies were also obtained at the MP2(full)/6-31G* level. All calculations used five-component *d* sets and seven-component *f* sets.

The above procedure reproduces our previous calculations for Gly [10], Ala [20], Ser, Cys and Pro [13], except for two differences: (a) the present results replace HF/6-31G* with MP2(full)/6-31G* geometries and vibrational frequencies, which leads to very minor changes on the computed binding enthalpies;

(b) no BSSE correction is applied, leading to binding enthalpies which are larger than the ones corrected by the full counterpoise method by 8–12 kJ mol^{-1}, depending on whether sodium ion complexation is mono-, bi- or tri-dentate. The accuracy of this computational level was checked by comparing the binding enthalpies resulting for the Na^+ complexes of acetamide and serine to those obtained at higher levels of theory. With both complexes, the basis set for final energetics was extended to aug-cc-pVTZ for H, C, N and O and aug-cc-pCVTZ for Na [46]. For acetamide, the geometry was optimized at the MP2/6-31+G* level, and final energetics led to an enthalpy of binding to Na^+ of 158.2 kJ mol^{-1}, i.e., 3 kJ mol^{-1} higher than the MP2/6-311+G(2d, 2p)//MP2/6-31G* value. For serine, the MP2/6-31G* geometry was retained, and the improved level yielded a correction of only −1 kJ mol^{-1} on the final enthalpy. These results indicate that the level used provides satisfactory accuracy without the need for BSSE corrections. Typical accuracies of the calculated values are ±4 kJ mol^{-1} for ΔH_{Na} and ±8 J mol^{-1} K^{-1} for ΔS_{Na}. All computations were carried out using the Gaussian 98 program package [47].

3. Results and discussion

3.1. Na^+ affinity order of amino acids

The CAD spectra of more than fifty AA_1–Na^+–AA_2 heterodimers were evaluated; ca. thirty of them exhibited acceptable signal:noise ratio and detectable abundances for both sodiated monomers, i.e., AA_1–Na^+ and Na^+–AA_2. Two representative spectra, corresponding to Gly–Na^+–Ala and Ala–Na^+–Val, are depicted in Fig. 1. Most dimer precursor ions undergo only the competitive decompositions leading to the metalated monomers (as those in Fig. 1). A few dimers produce additional, minor products upon CAD, involving the loss of H_2O (from Ala–Na^+–Ile and Gln–Na^+–His), NH_3 (Asp–Na^+–Tyr, Gln–Na^+–His, Glu–Na^+–Tyr and Gln–Na^+–Trp), CO_2 (Asn–Na^+–Gln) and CO+H_2O (Asp–Na^+–Tyr and Glu–Na^+–Tyr).

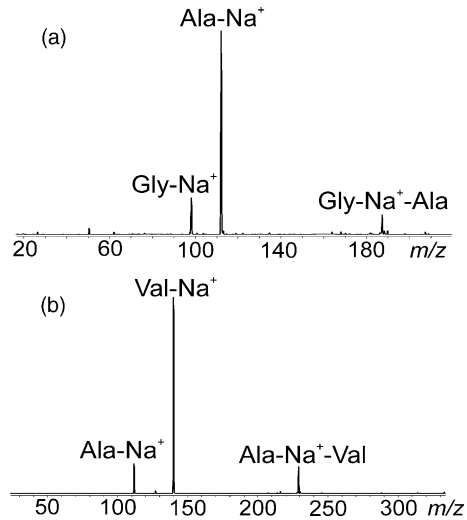

Fig. 1. CAD mass spectra of (a) Gly–Na^+–Ala (*m*/*z* 187) and (b) Ala–Na^+–Val (*m*/*z* 229) heterodimers.

The minor fragments suggest that CAD induces condensation reactions in a small population of AA_1–Na^+–AA_2, especially when side-chain functionalized amino acids are present. The relative abundances of the minor fragments are very sensitive to ESI and activation conditions, in contrast to the abundance ratio of AA_1–Na^+ vs. Na^+–AA_2, which is much less dependent on these variables and quite reproducible even within months (see below for standard deviations); hence, the minor CAD products do not influence significantly the $\ln(k_1/k_2)$ values from which the relative Na^+ affinities are derived.

A peculiar fragmentation pattern is observed in the CAD spectrum of the Ser–Na^+–Met heterodimer (Fig. 2). In addition to the expected sodiated monomers, which appear at *m*/*z* 128 and 172, respectively, this spectrum contains an abundant peak at *m*/*z* 150 (basepeak), nominally corresponding to protonated methionine, i.e., Met–H^+, and/or the Na^+ adduct of the sodium salt of serine, i.e., [Ser − H + Na]–Na^+. The MS/MS/MS spectrum [28] of *m*/*z* 150 is consistent with the latter composition and differs substantially from the reference CAD spectrum of protonated methionine (not shown). Based on these experiments, the *m*/*z* 150 fragment ion in Fig. 2 consists entirely of

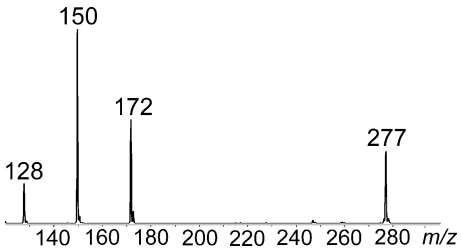

Fig. 2. CAD mass spectrum of Met–Na^+–Ser heterodimer (*m/z* 277). The *m/z* 150 fragment indicates contamination with the isobaric Na^+-bound homodimer of the sodium salt of serine, [Ser − H + Na]–Na^+–[Ser − H + Na]$^+$ (see text).

[Ser − H + Na]–Na^+, which indicates contamination of the Ser–Na^+–Met precursor ion by the isobaric homodimer [Ser − H + Na]–Na^+–[Ser − H + Na]. The described problem, compounded by the fact that Met could only be paired with Ser under the ESI conditions employed, prevented us from assessing the relative Na^+ affinity of Met.

A sufficient number of AA_1–Na^+–AA_2 dimers gave rise to useable CAD spectra, allowing for the construction of a Na^+ affinity ladder for sixteen of the twenty common α-amino acids. The ladder is presented in stair-step form in Fig. 3. The amino acid pairs compared in Na^+-bound dimers are connected by arrows, at which the corresponding $\ln(k_1/k_2)$ ratios are labeled; k_1 was assigned to the dissociation yielding the more abundant sodiated monomer, in order to obtain consistently positive $\ln(k_1/k_2)$ ratios. From the individual, experimental $\ln(k_1/k_2)$ data, average cumulative $\ln(k_{AA}/k_{Gly})$ values were calculated through a least-squares procedure; these are included in Fig. 3 and enable a quantitative assessment of the Na^+ binding energy of any given amino acid relative to glycine. Based on the reproducibility of relative abundances in the CAD spectra, the absolute errors of individual $\ln(k_1/k_2)$ values lie within 0.10 ± 0.10; Fig. 3 gives the convoluted errors resulting upon buildup of the $\ln(k_{AA}/k_{Gly})$ scale.

Several AA_1 molecules could be paired with more than one AA_2. In these cases, it is possible to reach a certain $\ln(k_1/k_2)$ ratio via different routes. We generally find very good agreement between $\ln(k_1/k_2)$

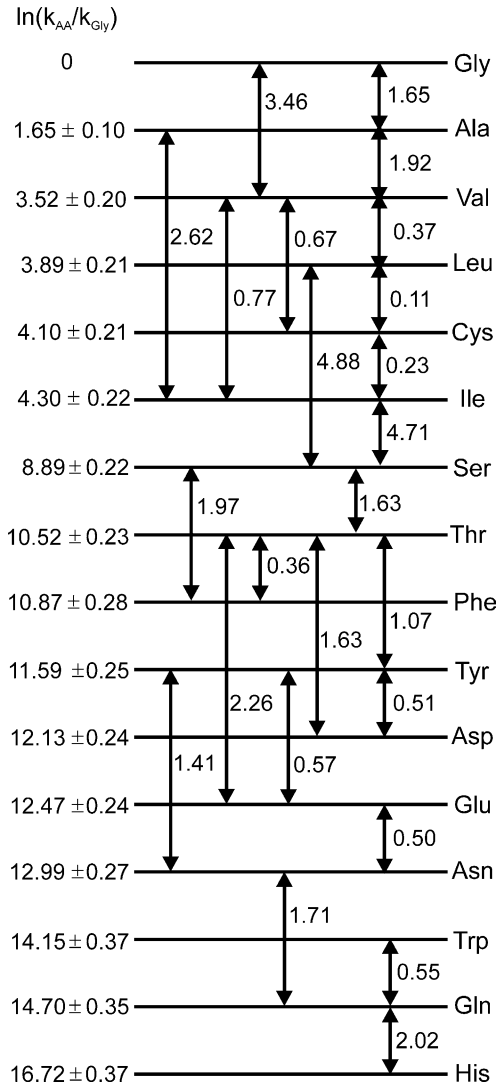

Fig. 3. Ln(k_1/k_2) ladder for Na^+-bound amino acid dimers, AA_1–Na^+–AA_2. The k_1/k_2 ratios were calculated from the abundances of AA_1–Na^+ and AA_2–Na^+ in CAD spectra. The AA_1/AA_2 pairs of the dimers investigated are connected by arrows. The data presented under the heading $\ln(k_{AA}/k_{Gly})$ are average cumulative values relative to Gly and include the numbers in parenthesis give the compounded error limits resulting from the reproducibility of relative abundances. The ladder does not include the $\ln(k_1/k_2)$ values of Lys–Na^+–Trp (1.02 ± 0.10) and Arg–Na^+–His (1.85 ± 0.10) which are subject to entropy effects and provide only lower limits for Lys and Arg; the resulting cumulative $\ln(k_{AA}/k_{Gly})$ values are $>15.17 \pm 0.38$ and $>18.57 \pm 0.38$, respectively.

data obtained in one vs. several steps. For example, $\ln(k_{Ile}/k_{Ala})$ measured directly (2.62 ± 0.05) agrees within experimental error (cf. Fig. 3) with the value calculated by summing $\ln(k_{Ile}/k_{Val})$ and $\ln(k_{Val}/k_{Ala})$, viz. 2.69(±0.06) = 0.77(±0.04)+1.92(±0.04). Similarly, the direct comparison of Asp and Thr renders 1.63 (±0.10), which is in accord with the cumulative $\ln(k_{Asp}/k_{Thr})$ of 1.58 (±0.10) obtained by comparing first Tyr to Thr (1.07 ± 0.10) and then Asp to Tyr (0.51 ± 0.03). The largest discrepancy in the $\ln(k_1/k_2)$ scale of Fig. 3 is found for the ranking of Glu vis à vis Thr, with the Glu–Na^+–Thr dimer leading to 2.26 (±0.06) but the stepwise comparison via Glu–Na^+–Tyr (0.57±0.02) and Tyr–Na^+–Thr (1.07± 0.10) to 1.64 (±0.10); nonetheless, both these values place Glu between Asp and Asn and their difference adds an uncertainty of only ca. 1–2 kJ mol^{-1} to the relative Na^+ affinity of Glu (vide infra).

Previous computational and experimental studies indicated that the amino acids listed in Fig. 3 preferentially form charge-solvated complexes with Na^+ [10–14,16–20]. Pro, which was not included in the ladder of Fig. 3, is an exception, binding Na^+ differently, viz. through a salt bridge [13,20]. In order to inquire whether this structural change would cause Pro–Na^+–AA dimers to produce inconsistent $\ln(k_1/k_2)$ data, we compared Pro to five amino acids (Ser, Thr, Tyr, Asp and Asn), and the resulting $\ln(k_1/k_2)$ ladder is displayed separately in Fig. 4. The Pro dimers with Ser, Thr, Asp and Asn invariably set the Na^+ affinity of Pro between those of Ser and Thr. There is very good agreement between cumulative and added sequential $\ln(k_1/k_2)$ values in these cases; for example, $\ln(k_{Asn}/k_{Pro})$ = 2.66 (±0.20) matches within experimental error the sum of $\ln(k_{Thr}/k_{Pro})$ + $\ln(k_{Tyr}/k_{Thr})$ + $\ln(k_{Asn}/k_{Tyr})$ = 0.44(±0.04) + 1.07(±0.10) + 1.41(±0.12) = 2.92(±0.16). In contrast, the dimer of Pro and Tyr suggests that the Na^+ affinity of Pro lies between those of Thr and Tyr and the respective $\ln(k_{Tyr}/k_{Pro})$ ratio (0.78 ± 0.08) differs markedly from the one predicted by combining the ratios of the Thr/Pro and Tyr/Thr pairs: 0.44(±0.04) + 1.07(±0.10) = 1.51(±0.11). The conflicting behavior of the Tyr–Na^+–Pro dimer could originate from

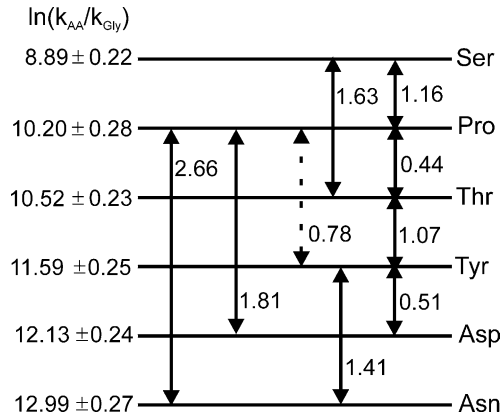

Fig. 4. Ln(k_1/k_2) ladder for Na^+-bound amino acid dimers composed of Pro and Ser, Thr, Tyr, Asp, or Asn. The data presented under the heading $\ln(k_{AA}/k_{Gly})$ are average cumulative values relative to Gly and include the compounded error limits resulting from the reproducibility of relative abundances. The dashed arrow identifies the AA_1–Na^+–AA_2 dimer whose $\ln(k_1/k_2)$ value is inconsistent (see text).

entropy effects. It is difficult to discern, however, why such effects are not duplicated with other Pro containing heterodimers. An alternative explanation could be that the Tyr–Na^+–Pro dimer produced upon ESI has a distinct structure, that is not formed when Pro is paired with other amino acids. Unfortunately, no hints on this scenario are provided by the CAD spectra, in all of which the sodiated monomers are the only significant fragments. For an appraisal of the Na^+ affinity of Pro relative to Gly, the deviating dimer was excluded. The four remaining dimers yield an average cumulative $\ln(k_{Pro}/k_{Gly})$ value of 10.20 ± 0.28 (Fig. 4) and the order Ser < Pro < Thr. Inclusion of the outlying result does not affect this order and results in a very similar value for $\ln(k_{Pro}/k_{Gly})$ of 10.32 ± 0.28.

Thirteen of the seventeen amino acids listed in Figs. 3 and 4 could be examined in at least three and up to six heterodimers. The overall acceptable self-consistency of the experimental data in these cases lends support to the assumption that the majority of amino acids have comparable apparent Na^+ binding entropies and that the apparent relative entropy of the bonds compared in AA_1–Na^+–AA_2 is negligible, for appreciable apparent relative entropies

tend to be non-additive and cause severe disparities between one-step and cumulative $\ln(k_1/k_2)$ ratios [35,36,40,43].

With the amino acids Lys and Arg, the only dimers that gave acceptable CAD spectra were Lys–Na^+–Trp and Arg–Na^+–His. The corresponding $\ln(k_1/k_2)$ values (see Fig. 3) convey the Na^+ affinity order Trp < Gln < Lys < His < Arg and place Lys and Arg at 15.17 ± 0.38 and 18.57 ± 0.38, respectively, in the cumulative $\ln(k_1/k_2)$ scale vs. glycine. The basic side-chain substituents of Lys and Arg most likely participate in the coordination of metal ions, as shown by theory for the $[Arg + Na]^+$ complex [14]. Because the side chains of Lys and Arg are much longer than those of other functionalized amino acids, the Na^+ binding entropies of Lys and Arg are expected to be substantially higher compared to those of other AA molecules; such a trend has been reported for the copper(I) and silver ion complexes of Lys and Arg [40,42,43]. The unequal entropies of the metal ion-ligand bonds in Lys–Na^+–AA and Arg–Na^+–AA dimers can cause considerable differences in the apparent Na^+ binding entropies of Lys vs. AA or Arg vs. AA, leading to underestimated relative affinities for Lys and Arg (because the experiment probes $\Delta G = \Delta H - T_{eff}\,\Delta S^{app}$, cf. Eq. (3) [35,36]). The cumulative $\ln(k_{Lys}/k_{Gly})$ and $\ln(k_{Arg}/k_{Gly})$ values quoted above should, therefore, be regarded as lower limits of the Na^+ binding energies (ΔH) of lysine and arginine relative to glycine.

3.2. Relative affinities anchored to Ala–Na^+

Conversion of the $\ln(k_1/k_2)$ ladders of Figs. 3 and 4 to a scale of relative Na^+ affinities in kJ mol^{-1} necessitates knowledge of the effective temperature (T_{eff}) of the AA_1–Na^+–AA_2 dimers at the activation conditions used. This can be achieved by the examination of AA–Na^+–B_i dimers composed of a suitable amino acid and a series of chemically similar reference bases of known Na^+ affinity (B_i). The B_i set must form dimers with AA, which dissociate to yield both AA–Na^+ and Na^+–B_i. These requirements could be met with the Na^+-bound dimers of Ala and the three aliphatic amides listed in Table 1, whose Na^+ affinities (ΔH_{298}) were calculated by ab initio theory; we did not utilize existing experimental data, assessed via threshold collision-induced dissociation [22], because these vary over a wide range depending on the parameters selected to correct for kinetic shifts (Table 1).

$$\ln\left(\frac{k_{Ala}}{k_{B_i}}\right) = \frac{\Delta H_{Na}(Ala) - T_{eff}\,\Delta(\Delta S_{Na})^{app}}{RT_{eff}} - \frac{\Delta H_{Na}(B_i)}{RT_{eff}} \quad (4)$$

$$\text{slope} = -\frac{1}{RT_{eff}} \quad (5)$$

$$x\text{-intercept} = \Delta H_{Na}(Ala) - T_{eff}\,\Delta(\Delta S_{Na})^{app} \approx \Delta H_{Na}(Ala) \quad (6)$$

The study of Ala–Na^+–B_i provides both T_{eff} as well as the absolute Na^+ affinity (ΔH_{Na}) of alanine, which then can be used to anchor the relative affinities of the other amino acids. Application of Eq. (3) to Ala–Na^+–B_i heterodimers results into Eq. (4). The k_{Ala}/k_{B_i} ratios are determined from the CAD spectra of Ala–Na^+–B_i, which were measured at four different collision energies, corresponding to four different effective temperatures [36,48]. The spectrum of Ala–Na^+–$CH_3CONHCH_3$ obtained with a resonance excitation amplitude (V_{p-p}) of 0.5 V is depicted in Fig. 5. A plot of the $\ln(k_{Ala}/k_{B_i})$ ratios at each collision energy against $\Delta H_{Na}(B_i)$ yields four regression lines, such as the one shown in Fig. 6, which refers to a V_{p-p} of 0.5 V. The slope, Eq. (5), and x-intercept, Eq. (6),

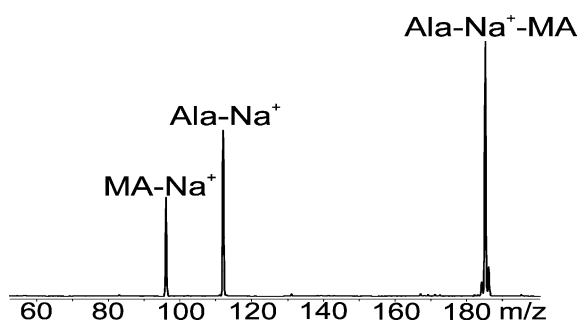

Fig. 5. CAD mass spectrum of the Na^+-bound dimer of alanine and *N*-methylacetamide (MA), Ala–Na^+–MA (*m/z* 185).

Table 1
Na^+ affinities (in kJ mol^{-1}) and complexation entropies (in J mol^{-1} K^{-1}) of the reference bases (B_i) used in the determination of the Na^+ affinity of alanine

B_i	ΔH_{Na} (298 K) (MP2(full)/6-311+G(2d,2p)// MP2/6-31G*)	ΔH_{Na} (298 K) (Exp.[a])	ΔS_{Na} (298 K) (MP2/6-31G*)
CH_3CONH_2 acetamide	155.6	145.2, 145.2, 145.2	102.5
$CH_3CONHCH_3$ *N*-methylacetamide	164.4[b,c], 165.3[b,c]	163.2, 141.0, 149.4	107.5[b], 90.8[b]
$CH_3CON(CH_3)_2$ *N,N*-dimethylacetamide	168.6	195.4, 147.3, 156.9	86.6

[a] Using threshold collision-induced dissociation [22]. The first number is uncorrected for kinetic shifts (±10 kJ mol^{-1}). The second and third numbers result after correcting for kinetic shifts with a different value of the two lowest frequencies of the transition state.
[b] Amide methyl group pointing toward or away from Na^+.
[c] The mean value of 164.9 kJ mol^{-1} was used for plots according to Eq. (4).

of the regression line in Fig. 6 and the lines obtained similarly at the other collision energies are summarized in Table 2. These slopes and intercepts provide information about T_{eff} and ΔH_{Na}(Ala), respectively. It is evident from Table 2 that the *x*-intercepts do not change appreciably with T_{eff} (i.e., with the collision energy). Thus, it appears that the differences in the apparent entropies of Na^+ binding for these systems (i.e., $\Delta(\Delta S_{Na})^{app}$) are quite small. Under these conditions, the *x*-intercepts directly provide the Na^+ affinity of alanine according to Eq. (6). The value derived, $\Delta H_{Na}(Ala) = 166.8$ kJ mol^{-1}, is based on the 298 K affinities of B_i (Table 1) and, hence, also corresponds to a 298 K affinity; it is assigned an error of ±5 kJ mol^{-1}, mainly reflecting the uncertainty in $\Delta H_{Na}(B_i)$.

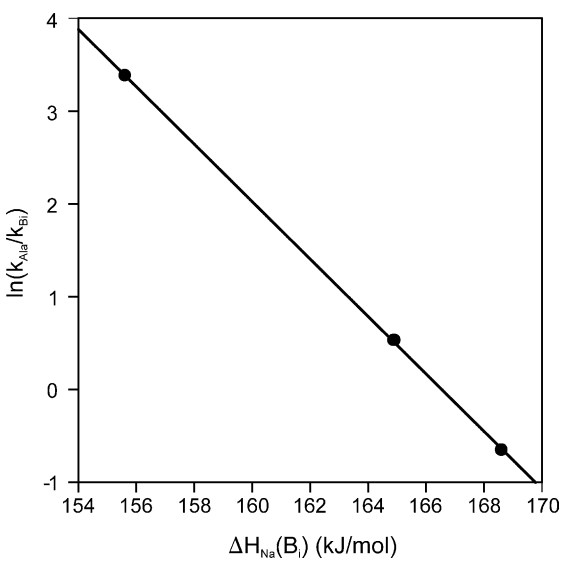

Fig. 6. Plot of $\ln(k_{Ala}/k_{B_i})$ vs. $\Delta H_{Na}(B_i)$ for heterodimers Ala–Na^+–B_i; B_i is the set of aliphatic amides listed in Table 1. The k_{Ala}/k_{B_i} ratios were calculated from the abundances of Ala–Na^+ and B_i–Na^+ in CAD spectra of Ala–Na^+–B_i ($V_{p-p} = 0.5$ V). The relationship between $\ln(k_{Ala}/k_{B_i})$ and $\Delta H_{Na}(B_i)$ is given in Eq. (4); the correlation coefficient of the regression line (r^2) is 0.999.

It is worth noting that the average thermodynamic entropy of the B_i–Na^+ bonds, $\Delta S_{Na}(B_i)_{avg} = 97 \pm 10$ J mol^{-1} K^{-1} (Table 1), is distinct from the thermodynamic entropy of the Ala–Na^+ bond (117 J mol^{-1} K^{-1} [20]). As mentioned earlier, the experiment probes the apparent quantity $\Delta(\Delta S_{Na})^{app}$, not the actual $\Delta(\Delta S_{Na})$ difference. Generally, $\Delta(\Delta S)^{app} \approx 0$ if $\Delta(\Delta S) \approx 0$ [35,36]. On the other hand, our result with the Ala–Na^+–B_i dimers and other studies [35,36] have demonstrated that a negligible or very small $\Delta(\Delta S)^{app}$ may correspond to a sizable $\Delta(\Delta S)$; consequently, apparent relative entropies from kinetic method experiments should not be used to determine absolute thermodynamic entropy data.

The average collision energy (V_{p-p}) in the CAD experiments of Ala–Na^+–B_i, 0.55 ± 0.13 V, is very similar with that used for CAD of the AA_1–Na^+–AA_2 heterodimers (0.55 ± 0.17 V). Collision energies determine the internal energy deposited into the dimer ions. The effective temperature gauges the latter energy, but also depends on experimental conditions [30,49,50]; since the CAD spectra of Ala–Na^+–B_i and AA_1–Na^+–AA_2 were acquired under constant

Table 2
Effective temperature, T_{eff}, of Ala–Na^+–B_i dimers activated at different collision energies, and sodium ion affinity of alanine, ΔH_{Na}(Ala), deduced from CAD of Ala–Na^+–B_i according to Eq. (4)

	Collision energy, V_{p-p} (V)[a]			
	0.4	0.5	0.6	0.7
Slope of Eq. (4)[b]	−0.318 (0.022)	−0.309 (0.003)	−0.291 (0.002)	−0.247 (0.025)
T_{eff} from Eq. (5) (K)[c]	378	389	413	487
x-Intercept of Eq. (4)[b]	166.4 (0.4)	166.5 (0.1)	167.4 (0.1)	166.9 (0.7)
ΔH_{Na}(Ala) from Eq. (6) (kJ mol^{-1})	Mean value of x-intercept = 166.8			

[a] The linear correlation coefficients (r^2) of the regression lines are 0.995 (0.4 V), 0.999 (0.5 V), 0.999 (0.6 V) and 0.990 (0.7 V).
[b] The numbers in parentheses give standard deviations.
[c] The mean value of the four slopes, 0.291 (0.032), corresponds to a mean effective temperature of 413 (45) K.

experimental conditions, T_{eff} of AA_1–Na^+–AA_2 should lie within the range of effective temperatures measured for Ala–Na^+–B_i, which is 413 ± 45 K (cf. Table 2). This value was utilized to calculate via Eq. (3) the Na^+ affinities of amino acids relative to Gly, $\Delta H_{Na}(AA)–\Delta H_{Na}(Gly) = \Delta(\Delta H_{Na})$, from the cumulative $\ln(k_1/k_2)$ ratios discussed in the previous section and included in Figs. 3 and 4. Gly was chosen as the reference point of relative affinities because it is the AA with the smallest Na^+ binding energy. The ensuing scale is presented in Table 3, which also contains the absolute Na^+ affinities obtained by anchoring the relative values to ΔH_{Na}(Ala) = 166.8 kJ mol^{-1}. The uncertainty in T_{eff} (±45 K) and abundance ratios (less or equal than ±0.37 in $\ln(k_1/k_2)$ units, cf. Figs. 3–4) introduce an error of ±1–6 kJ mol^{-1} in the relative Na^+ affinities (average error ±4 kJ mol^{-1}); this error mainly originates from the uncertainty in T_{eff}, which uniformly affects all relative affinities and does not modify the affinity order. The error in absolute affinities, which is convoluted by the added uncertainty in $\Delta H_{Na}(B_i)$, is estimated at ±8 kJ mol^{-1}.

The Na^+ affinities of Gly, Ala, Pro, Cys and Ser were also calculated by ab initio methods (Table 3). As has been mentioned, the lowest-energy structure of $[Pro + Na]^+$ contains the proline zwitterion (i.e., a salt bridge) [13,20], while those of the other four $[AA + Na]^+$ ions involve metal ion solvation by the free acid form of AA in a bidentate (Gly, Ala) or tridentate (Cys, Ser) fashion [7–13,15–20]. The selected complexes are thus representative systems of the metal ion coordination modes possible with AA ligands. In all five cases the concert between our experimental and ab initio affinities is very good to excellent (Table 3). The kinetic method measurements do not reproduce the theoretically predicted order Cys < Pro < Ser (they suggest Cys < Ser < Pro), but calculated and experimental ΔH_{Na} do not disagree beyond their error limits (±4 and ±8 kJ mol^{-1}, respectively). Interestingly, the Na^+ affinities of Gly, Ala, Phe, Tyr and Trp calculated by density functional theory using a smaller basis set and BSSE corrections [16,17] are very similar to our high-level MP2 and kinetic method values (Table 3).

Our ΔH_{Na}(Ala) agrees well with the affinity reported by Bojesen et al. (165 kJ mol^{-1}), which is rather coincidental considering the arbitrary manner in which the latter value was estimated [21]; the Na^+ affinity of Ala deduced here also is in fair agreement with a recent value measured by ligand exchange equilibria (159 kJ mol^{-1} [23]). A significant discrepancy is, however, observed between our new Na^+ affinities of the aromatic amino acids Phe, Tyr and Trp and older values from our laboratory, obtained via the kinetic method with FAB-generated AA–Na^+–nucleobase dimers [17]. The new data (Table 3) reveal a relative affinity of 31 ± 4 kJ mol^{-1} between Phe and Ala; in contrast, the previous study [17] reported 9 ± 8 kJ mol^{-1}, while an independent investigation of the relative Na^+ affinity of Ala/Phe via stepwise ligand exchange equilibria has yielded a difference of 29 ± 8 kJ mol^{-1} [23]. On the basis of these comparisons,

Table 3
Sodium ion affinities of common α-amino acids (AA). Proton affinities and relative copper(I) ion affinities are included for comparison. All data are in kJ mol^{-1}

AA	$\Delta(\Delta H_{Na})$ (this study)	ΔH_{Na} (this study)		ΔH_{Na}		PA[a]	$\Delta(\Delta H_{Cu})$[b]
	Exp.[c]	Exp.[d]	Calc.[e]	Exp.	Calc.		
Gly	0.0	161	164	159[f], 153[g]	168[h]	887	0.0
Ala	5.7	167	167	165[f], 159[i]	170[h]	902	7.1
Val	12.1	173		172[f]		911	15.5
Leu	13.4	175				915	17.2
Cys	14.1	175	180			903	36.0
Ile	14.8	176				917	18.0
Ser	30.5	192	200			915	13.0
Pro	35.0	196	195			921	20.1
Thr	36.1	197				923	19.2
Phe	37.3	198		174[j], 188[i]	201[h]	923	33.5
Tyr	39.8	201		175[j]	202[h]	926	34.7
Asp	41.7	203				909	20.9
Glu	42.8	204				913	30.1
Asn	44.6	206				929	28.0
Trp	48.6	210		180[j]	218[h]	949	48.1
Gln	50.5	212				938	41.0
Lys	>52.1[k]	>213				996	87.5[l]
His	57.4	219				988	55.6
Arg	>63.8[k]	>225				1051	96.5[l]

[a] [25].
[b] [40].
[c] Relative Na^+ affinities based on Figs. 3–4 (±4 kJ mol^{-1}).
[d] Absolute Na^+ affinities, anchored to the value of Ala (±8 kJ mol^{-1}).
[e] MP2(full)/6-311+G(2d,2p)//MP2/6-31G* without BSSE corrections. The Na^+ binding entropies computed at the MP2/6-31G* level are (in J mol^{-1} K^{-1}): Gly, 116; Ala, 117; Cys, 124; Pro, 109; Ser, 123. The uncertainties in the calculated enthalpies and entropies are estimated at ±4 kJ mol^{-1} and ±8 J mol^{-1} K^{-1}, respectively.
[f] Using the kinetic method, [21].
[g] Using threshold collision-induced dissociation, [22].
[h] B3LYP/6-31+G(d) with BSSE corrections, [16,17].
[i] Using ligand exchange equilibria, [23].
[j] Using the kinetic method, [17].
[k] Lower limits due to considerable activation entropies of Na^+ binding, see text.
[l] With consideration of activation entropies of Cu^+ binding, [42].

it is concluded that absolute and relative Na^+ affinities of the aromatic amino acids were underestimated in our FAB-kinetic method experiments. It is noteworthy that the ΔH_{Na} values of Gly, Ala and Val determined here using ESI-generated heterodimers of amino acids (161, 167 and 173 kJ mol^{-1}, respectively) match within experimental error those of Bojesen et al. who employed FAB-generated heterodimers of amino acids (159, 165 and 172 kJ mol^{-1}, respectively). The latter results suggest that the ligand paired with AA in the heterodimer (nucleobases vs. other amino acids) rather than the ionization technique (FAB vs. ESI) causes the underestimation. Perhaps, the rigid and bulky nucleobase ligands used in the earlier study, viz. adenine, cytosine and guanine [17], prevented the formation of heterodimers (with aromatic amino acids), from which the most stable $[AA + Na]^+$ complexes could be produced upon dissociation. Experiments examining this problem are currently under way in our laboratory.

Our calculations indicate that the entropies of Na^+ complexation of Gly, Ala, Pro, Cys and Ser are quite

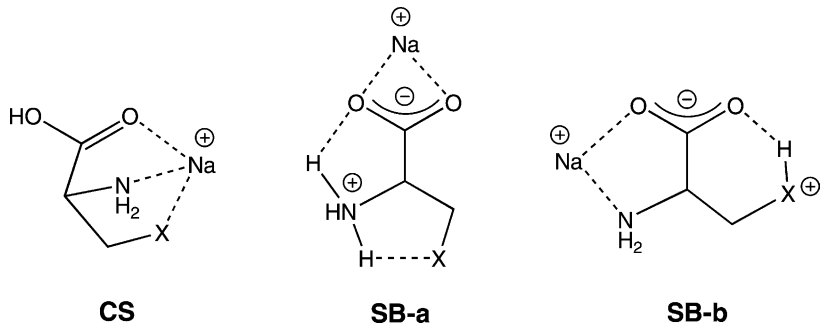

Fig. 7. Charge-solvated (**CS**) and salt-bridged (**SB-a** and **SB-b**) structures predicted by quantum chemical methods for the Na^+ complexes of side-chain functionalized amino acids [13,14,20]. X represents a heteroatom-carrying substituent. The most basic site of the amino acid is the amine group in **SB-a** and the X group in **SB-b**.

similar and that the relative entropies among them are small (see footnote c in Table 3). The corresponding apparent relative entropies, which tend to be smaller than thermodynamic relative entropies [35,36] are thus negligible, as assumed above and corroborated by the self-consistency of one-step and cumulative $\ln(k_1/k_2)$ values in the ladders of Figs. 3–4. From the seventeen amino acids contained in these ladders, Gly, Phe, Trp and His could not be examined in at least three heterodimers to unequivocally confirm that their apparent Na^+ binding entropies are similar to those of the other AA molecules. The accord between our experimental ΔH_{Na} of Gly, Phe and Trp and the calculated Na^+ affinities obtained by us (for Gly) or others (for Phe and Trp [16,17]) strongly suggests that the apparent relative entropies of the Gly, Phe and Trp heterodimers investigated are indeed negligible. Only the apparent Na^+ binding entropy of His could not be cross-checked by self-consistency tests or calculations; for this reason, the Na^+ affinity of His reported in Table 3 might be underestimated due to entropy effects, as explained for Lys and Arg (vide supra).

3.3. Comparison of Na^+ with H^+ and Cu^+ affinity orders

Charge-solvated and zwitterionic geometries are possible for the $[AA + Na]^+$ complexes. Three relevant arrangements are illustrated in Fig. 7 for a side-chain functionalized amino acid. The isomers with salt bridges (**SB-a** and **SB-b**) have a proton attached to the most basic site. If such "protonated" structures were probed in our experiments, the sodium ion affinities of amino acids should correlate well with the corresponding proton affinities (PA) [15]. The data of Table 3 and the plot of Fig. 8 attest, however, that this is not true. The poor correlation observed is instead consistent with charge solvation as the predominant mode of Na^+ complexation by AA (**CS**) [20]. In charge-solvated complexes, bonding results from noncovalent electrostatic interactions, which are fundamentally different from the covalent bonds formed by protons. This difference in AA–Na^+ (**CS**) vs. AA–H^+ bonding justifies the lack of a relationship between PA and ΔH_{Na}.

The Na^+ affinities do not correlate with the respective Cu^+ affinities as well (cf. Table 3 and Fig. 9). This result can be explained by the hard/soft acid/base principle [51,52]. Na^+ is a hard Lewis acid, while Cu^+ is a soft Lewis acid. Consequently, the former ion interacts most favorably with hard Lewis bases (such as hydroxy- and carbonyl-substituted amino acids), while the latter ion prefers interactions with soft Lewis bases (such as the thiol group of Cys) [40]. A further reason for the deviating affinity orders of the two metal ions is that, unlike Na^+ ion, Cu^+ ion can undergo s-d hybridization; such hybridization is most effective in bidentate complexes, in which the two binding sites attach at 180° to the transition metal ion [53].

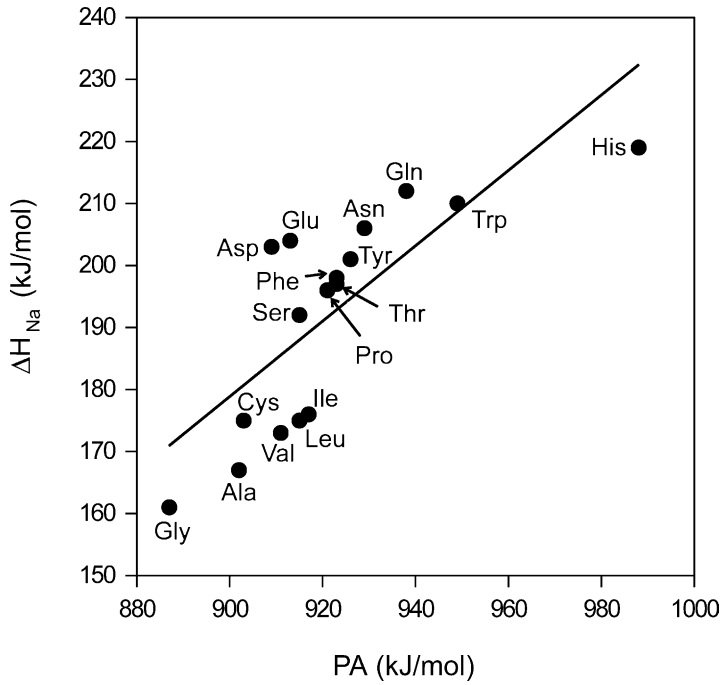

Fig. 8. Plot of the sodium ion affinities of amino acids, ΔH_{Na}, vs. the corresponding proton affinities, PA (Table 3). The solid line is a least-square fit to the data ($r^2 = 0.601$).

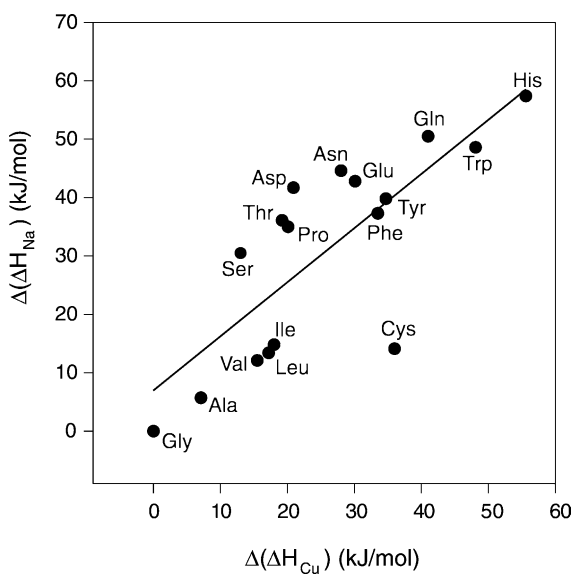

Fig. 9. Plot of the relative sodium ion affinities of amino acids, $\Delta(\Delta H_{Na})$, vs. the corresponding copper(I) affinities, $\Delta(\Delta H_{Cu})$ (Table 3). The solid line is a least-square fit to the data ($r^2 = 0.609$).

Extending an amino acid side chain to accommodate more easily a 180° (i.e., linear) arrangement, should thus improve Cu^+ affinities much more than Na^+ affinities; this is substantiated by the affinity increases from Asp to Glu and from Asn to Gln, which are markedly larger for Cu^+ than Na^+ (Table 3 and Fig. 9).

3.4. Side-chain substituent effects

Amino acids with functional side chains generally bind Na^+ more strongly than aliphatic amino acids (Table 3). The increased Na^+ affinity of the functionalized molecules strongly suggests that the side-chain substituent participates in the coordination of the metal ion, enhancing the stability of the $[AA + Na]^+$ complex. There are two notable exceptions to this trend. The bond energy of the $[Cys + Na]^+$ complex falls within the range observed for aliphatic $[AA + Na]^+$ complexes, while the Pro–Na^+ bond energy resembles those of the markedly stronger Phe–Na^+ and Thr–Na^+ bonds.

The low Na^+ affinity of cysteine can be rationalized by the weak interaction expected between the hard Na^+ ion (acid) and the soft SH group of the cysteine side chain (base). Serine, in which the side-chain heteroatom is replaced by a much harder OH site, forms a 17 kJ mol^{-1} stronger bond with Na^+ (Table 3). The different Na^+ binding properties of Cys and Ser are reflected by the calculated structures of their Na^+ complexes [13]. In both, Na^+ is bound to the carbonyl, amine and side-chain groups (structure **CS** in Fig. 7). The $Na^+ \cdots SH$ bond in $[Cys + Na]^+$ (3.0 Å) is, however, much longer than the $Na^+ \cdots OH$ bond in $[Ser + Na]^+$ (2.4 Å); the other two bonds have very similar lengths in both complexes (all at 2.3–2.4 Å).

The high ranking of proline in the Na^+ affinity scale is attributed to the zwitterionic character of the Pro–Na^+ bond. Ab initio calculations have revealed that the high stability of zwitterionic $[Pro + Na]^+$ originates from the synergism of (a) the higher proton affinity of secondary vs. primary amines *and* (b) the nearly linear geometry of the $+-+$ charges of the salt bridge [13,20]. The angle between the $+-$ and $-+$ dipoles in salt bridges of side-chain functionalized amino acids deviates significantly from 180° (see, for example, **SB-a** and **SB-b** in Fig. 7) [20], which reduces the stability of the corresponding zwitterionic $[AA + Na]^+$ complexes. As shown by theory and experiment [13,14,20], a proton affinity above PA(Arg) is necessary in order for AA with functional side chains to form salt-bridged Na^+ complexes that are comparably stable with charge-solvated isomers.

The relative Na^+ affinities measured (Table 3) indicate that the strength of the electrostatic interaction between Na^+ and the side-chain substituent increases in the order SH (Cys) $\ll$ OH (Ser, Thr) $<$ phenyl (Phe, Tyr) $<$ COOH (Asp, Glu) $<$ $CONH_2$ (Asn, Gln) $<$ indolyl (Trp) $<$ imidazolyl (His). Amide and electron-rich aromatic groups are among the intrinsically strongest binding ligands. A more quantitative assessment of the Na^+-(side chain) contribution to the AA–Na^+ binding energy can be obtained by limiting comparisons to substituted alanines, i.e., to amino acids with the connectivity $H_2NCH(CH_2X)COOH$, where X represents the functional group of the side chain; the corresponding complexes have tridentate structures **CS** (Fig. 7), except for Ala itself which forms a bidentate complex. Based on the relative Na^+ affinities between alanine and its functionalized analogs, the increments in overall bond energy provided by the various $Na^+ \cdots X$ interactions rise as follows (numbers give $\Delta(\Delta H_{Na})$ in kJ mol^{-1}): H (in Ala; 0) $<$ SH (in Cys; 8) $<$ OH (in Ser; 25) $<$ phenyl (in Phe; 31) $<$ *p*-hydroxyphenyl (in Tyr; 34) $<$ COOH (in Asp; 36) $<$ $CONH_2$ (in Asn; 39) $<$ indolyl (in Trp; 43) $<$ imidazolyl (in His; 52).

4. Conclusions

The kinetic method has been used to deduce the relative Na^+ affinities of the common α-amino acids based on the dissociations of Na^+-bound heterodimers of different amino acids, and the absolute Na^+ affinity of alanine based on the dissociations of Na^+-bound dimers of Ala with aliphatic amides. The Na^+ affinities of the amide reference bases were determined by high-level ab initio theory. Calculations were also carried out on the Na^+ binding energies of Gly, Ala, Pro, Cys and Ser, in order to cross-check the quality of experimental and computational results. The relative and absolute values obtained by the kinetic method measurements agree very well with the quantum chemistry predictions. Our study provides first reliable Na^+ affinity data for the amino acids Val, Leu, Ile, Pro, Cys, Ser, Thr, Asp, Glu, Asn, Gln and His. For Gly and Ala, the Na^+ affinities reported here are in reasonable agreement with previous experimental data. On the other hand, substantially larger affinities are found for the aromatic amino acids Phe, Tyr and Trp, compared to earlier kinetic method experiments employing heterodimers with the nucleobases adenine, cytosine or guanine. The latter result is attributed to the sampling of less stable $[AA + Na]^+$ isomers in heterodimers with the rigid and bulky nucleobases.

Na^+ affinities of amino acids do not correlate well with the corresponding proton or copper(I) affinities.

This behavior arises from the different types of bonds formed by protons (covalent σ), Cu^+ ions (electrostatic with some covalent character) and Na^+ ions (purely electrostatic), as well as from the distinctive Lewis acid properties of the three cations. The relative Na^+ scale measured in this study reveals that strong binding interactions are developed between Na^+ and amino acid side chains that carry amide or electron-rich aromatic substituents.

Acknowledgements

We thank Kathleen M. Wollyung for experimental assistance, Dr. Michael J. Polce for helpful comments and the National Science Foundation (CHE-0111128) for generous financial support.

References

[1] S.J. Lippard, J.M. Berg, Principles of Bioinorganic Chemistry, University Science Books, Mill Valley, CA, 1994.
[2] W. Kaim, B. Schwederski, Bioinorganic Chemistry: Inorganic Elements in Chemistry of Life, Wiley, Chichester, 1994.
[3] D.J. Aidley, P.R. Stanfield, Ion Channels: Molecules in Action, Cambridge University Press, Cambridge, 1996.
[4] J.A. Cowan, Inorganic Biochemistry: An Introduction, 2nd ed., Wiley-VCH, New York, 1997.
[5] R.G. Cooks, J.S. Patrick, T. Kotiaho, S.A. McLuckey, Mass Spectrom. Rev. 13 (1994) 287.
[6] R.G. Cooks, P.S.H. Wong, Acc. Chem. Res. 31 (1998) 379.
[7] F. Jensen, J. Am. Chem. Soc. 114 (1992) 9533.
[8] S. Bouchonnet, Y. Hoppilliard, Org. Mass Spectrom. 27 (1992) 71.
[9] D. Yu, A. Rauk, D.A. Armstrong, J. Am. Chem. Soc. 117 (1995) 1789.
[10] S. Hoyau, G. Ohanessian, Chem. Eur. J. 4 (1998) 1561.
[11] T. Wyttenbach, J.E. Bushnell, M.T. Bowers, J. Am. Chem. Soc. 120 (1998) 5098.
[12] T. Wyttenbach, M. Witt, M.T. Bowers, Int. J. Mass Spectrom. 182/183 (1999) 243.
[13] S. Hoyau, K. Norrman, T.B. McMahon, G. Ohanessian, J. Am. Chem. Soc. 121 (1999) 8864.
[14] R.A. Jockusch, W.D. Price, E.R. Williams, J. Phys. Chem. A 103 (1999) 9266.
[15] T. Wyttenbach, M. Witt, M.T. Bowers, J. Am. Chem. Soc. 122 (2000) 3458.
[16] R.C. Dunbar, J. Phys. Chem. A 104 (2000) 8067.
[17] V. Ryzhov, R.C. Dunbar, B.A. Cerda, C. Wesdemiotis, J. Am. Soc. Mass Spectrom. 11 (2000) 1037.
[18] T. Marino, N. Russo, M. Toscano, J. Inorg. Biochem. 79 (2000) 179.
[19] T. Marino, N. Russo, M. Toscano, Inorg. Chem. 40 (2000) 6439.
[20] J.M. Talley, B.A. Cerda, G. Ohanessian, C. Wesdemiotis, Chem. Eur. J. 8 (2002) 1377.
[21] G. Bojesen, T. Breindahl, U.N. Andersen, Org. Mass Spectrom. 28 (1993) 1448.
[22] J.S. Klassen, S.G. Anderson, A.T. Blades, P. Kebarle, J. Phys. Chem. 100 (1996) 14218.
[23] A. Gapeev, R.C. Dunbar, J. Am. Chem. Soc. 123 (2001) 8360.
[24] B.A. Cerda, C. Wesdemiotis, Analyst 125 (2000) 657.
[25] E.P.L. Hunter, S.G. Lias, J. Phys. Chem. Ref. Data 27 (1998) 413.
[26] M. Yamashita, J.B. Fenn, J. Phys. Chem. 88 (1984) 4451.
[27] J.B. Fenn, M. Mann, C.K. Meng, S.F. Wong, Science 246 (1989) 64.
[28] S.A. McLuckey, G.J. Van Berkel, D.E. Goeringer, G.L. Glish, Anal. Chem. 66 (1994) 689A.
[29] K.J. Laidler, Chemical Kinetics, 3rd ed., Harper & Row Publishers, New York, 1987, p. 112.
[30] R.G. Cooks, J.T. Koskinen, P.D. Thomas, J. Mass Spectrom. 34 (1999) 85.
[31] P.B. Armentrout, M.T. Rodgers, J. Phys. Chem. A 104 (2000) 2238.
[32] B.A. Cerda, C. Wesdemiotis, J. Am. Chem. Soc. 118 (1996) 11884.
[33] B.A. Cerda, S. Hoyau, G. Ohanessian, C. Wesdemiotis, J. Am. Chem. Soc. 120 (1998) 2437.
[34] B.A. Cerda, C. Wesdemiotis, Int. J. Mass Spectrom. 189 (1999) 189.
[35] K.M. Ervin, J. Am. Soc. Mass Spectrom. 13 (2002) 435.
[36] I.-S. Hahn, C. Wesdemiotis, Int. J. Mass Spectrom. 222 (2003) 465.
[37] W.J. Moore, Physical Chemistry, 5th ed., Longman, London, 1972.
[38] G. Bojesen, J. Am. Chem. Soc. 109 (1987) 5557.
[39] Z. Wu, C. Fenselau, Rapid Commun. Mass Spectrom. 6 (1992) 403.
[40] B.A. Cerda, C. Wesdemiotis, J. Am. Chem. Soc. 117 (1995) 9734.
[41] S. Hoyau, G. Ohanessian, J. Am. Chem. Soc. 119 (1997) 2016.
[42] B.A. Cerda, C. Wesdemiotis, Int. J. Mass Spectrom. 185/186/187 (1999) 107.
[43] V.W.-M. Lee, H. Li, T.-C. Lau, R. Guevremont, K.W.M. Siu, J. Am. Soc. Mass Spectrom. 9 (1998) 760.
[44] T.B. McMahon, G. Ohanessian, Chem. Eur. J. 6 (2000) 2931.
[45] D. Feller, Chem. Phys. Lett. 322 (2000) 543.
[46] K.A. Peterson, D. Feller, private communication.
[47] M.J. Frisch, G.W. Trucks, H.B. Schlegel, G.E. Scuseria, M.A. Robb, J.R. Cheesemann, V.G. Zakrzewski, J.A. Montgomery Jr., R.E. Stratmann, J.C. Burant, S. Dapprich, J.M. Millam, A.D. Daniels, K.N. Kudin, M.C. Strain, O. Farkas, J. Tomasi, V. Barone, M. Cossi, R. Cammi, B. Mennucci, C. Pomelli, C. Adamo, S. Clifford, J. Ochterski, G.A. Petersson, P.Y. Ayala, Q. Cui, K. Morokuma, D.K. Malick, A.D. Rabuck, K.

Raghavachari, J.B. Foresman, J. Cioslowski, J.V. Ortiz, B.B. Stefanov, G. Liu, A. Liashenko, P. Piskorz, I. Komaromi, R. Gomperts, R.L. Martin, D.J. Fox, T. Keith, M.A. Al-Laham, C.Y. Peng, A. Nanayakkara, M. Challocombe, P.M.W. Gill, B.G. Johnson, W. Chen, M.W. Wong, J.L. Andres, C. Gonzalez, M. Head-Gordon, E.S. Replogle, J.A. Pople, Gaussian 98, Gaussian, Inc., Pittsburgh, PA, 1998.

[48] X. Cheng, Z. Wu, C. Fenselau, J. Am. Chem. Soc. 115 (1993) 4844.

[49] K. Vékey, J. Mass Spectrom. 31 (1996) 445.

[50] S.L. Craig, M. Zhong, B. Choo, J.I. Brauman, J. Phys. Chem. A 101 (1997) 19.

[51] R.G. Pearson, J. Am. Chem. Soc. 85 (1963) 3533.

[52] M.B. Smith, J. March, Advanced Organic Chemistry: Reactions, Mechanisms, and Structure, Wiley, New York, 2001.

[53] C.W. Bauschlicher, S. R Langhoff, H. Partridge, J. Chem. Phys. 94 (1991) 2068.